Deep bradycardia and heart block caused by inducible cardiac-specific knockout of the pacemaker channel gene *Hcn4*

Mirko Baruscotti[a], Annalisa Bucchi[a], Carlo Viscomi[b,c], Giacomo Mandelli[a], Giacomo Consalez[c], Tomaso Gnecchi-Rusconi[d], Nicola Montano[e], Karina Rabello Casali[f], Stefano Micheloni[a], Andrea Barbuti[a], and Dario DiFrancesco[a,1]

[a]Department of Biomolecular Sciences and Biotechnology, PaceLab and Centro Interuniversitario di Medicina Molecolare e Biofisica Applicata, Milano, Università degli Studi di Milano, 20133 Milan, Italy; [b]Unit of Molecular Neurogenetics, National Neurological Institute Carlo Besta, 20133 Milan, Italy; [c]Division of Neuroscience, DiBiT San Raffaele Scientific Institute, 20132 Milan, Italy; [d]Department of Cardiology, Merate Hospital, 23807 Merate, Italy; [e]Department of Clinical Sciences "L. Sacco," Università degli Studi di Milano, 20157 Milan, Italy; and [f]Institute of Cardiology of Rio Grande do Sul, 90620-001, Porto Alegre, Brazil

Cardiac pacemaking generation and modulation rely on the co-ordinated activity of several processes. Although a wealth of evidence indicates a relevant role of the I_f ("funny," or pacemaker) current, whose molecular constituents are the hyperpolarization-activated, cyclic nucleotide-gated (HCN) channels and particularly HCN4, work with mice where *Hcn* genes were knocked out, or functionally modified, has challenged this view. However, no previous studies used a cardiac-specific promoter to induce HCN4 ablation in adult mice. We report here that, in an inducible and cardiac-specific HCN4 knockout (ciHCN4-KO) mouse model, ablation of HCN4 consistently leads to progressive development of severe bradycardia (~50% reduction of original rate) and AV block, eventually leading to heart arrest and death in about 5 d. In vitro analysis of sinoatrial node (SAN) myocytes isolated from ciHCN4-KO mice at the mean time of death revealed a strong reduction of both the I_f current (by ~70%) and of the spontaneous rate (by ~60%). In agreement with functional results, immunofluorescence and Western blot analysis showed reduced expression of HCN4 protein in SAN tissue and cells. In ciHCN4-KO animals, the residual I_f was normally sensitive to β-adrenergic receptor (β-AR) modulation, and the permanence of rate response to β-AR stimulation was observed both in vivo and in vitro. Our data show that cardiac HCN4 channels are essential for normal heart impulse generation and conduction in adult mice and support the notion that dysfunctional HCN4 channels can be a direct cause of rhythm disorders. This work contributes to identifying the molecular mechanism responsible for cardiac pacemaking.

funny current | heart rate | sinoatrial node | atrioventricular node | chronotropism

The degree of complexity of the processes involved in pacemaking and their individual contributions is still a hotly debated issue (1, 2). Despite this complexity, and granting the fact that perturbation of any participating mechanism can affect rate, there is evidence for a functional specificity of "funny" (f)-channels in mediating generation and physiological control of pacemaker activity.

Native f-channels are encoded by four hyperpolarization-activated, cyclic nucleotide-gated channel genes (*Hcn1–4*), of which *Hcn4* is by far the most highly expressed in the cardiac pacemaker regions of different species (3–6). HCN4 contributes 80% of total HCN mRNA in rabbit and mouse sinoatrial node (SAN), the remaining 20% being a combination of HCN2 and HCN1, with species-dependent relative abundance (4, 5, 7–9). Evidence for the role of f/HCN4 channels in pacemaking relies on several experimental data (10):

i) The "funny" (I_f) current and pacemaker activity are correlated; i.e., functional expression of f-channels is restricted to pacemaking regions [SAN, atrioventricular node (AVN), and the ventricular conduction system], demonstrating a commitment to regulation of pacemaker activity. This correlation exists not only in the adult but also throughout development, such that the *Hcn4* channel gene is considered a "marker" of pacemaker tissue (11–13).

ii) Certain mutations of human HCN4 channels leading to loss-of-function defects are associated with arrhythmias, and in particular with bradycardia (10).

iii) Drugs acting as selective I_f blockers slow heart rate without other cardiovascular side effects (14).

In addition to these data, recent studies from HCN4 knockout mice have also been carried out. One study showed that mice with constitutive HCN4 knockout, either global or cardiac specific, die in utero at embryonic days 10.5–11.5, suggesting that *Hcn4* is necessary for the formation of the SAN (15). Cre-loxP methods were then used to induce knockout of HCN4 in adult mice. A study using a ubiquitous Cre-recombinase promoter resulted in ~75% current reduction and led to arrhythmia characterized by recurrent sinus pauses, but the mean basal rates of mutant and wild-type mice were similar. Also, HCN4-deficient mice were normally responsive to sympathetic stimulation (16). Similar results were obtained with another knockout model where an inducible Cre was inserted in-frame into the *Hcn4* start codon (17). According to the authors (17), this model led to efficient recombination in the cardiac conduction system only, despite the fact that HCN4 is strongly expressed in several brain areas (18, 19), an observation for which the authors found no ready explanation.

With the exclusion of the constitutive knockout (15), the other HCN4 knockout models (16, 17) showed only mild effects on cardiac automaticity and no alteration of rate control. Our study, carried out with an inducible and cardiac-specific HCN4 knockout mouse model, yields different results because cardiac selective reduction of the HCN4 current is consistently accompanied by progressive development of severe bradycardia and AV block, eventually leading to heart arrest and death of the animal.

According to our results, HCN4 channels are necessary for normal rhythm generation and conduction, and their function represents a key molecular mechanism for cardiac pacemaking.

Results

A tamoxifen (Tam)-inducible, cardiac-specific HCN4 knockout mouse model based on the Cre-loxP system was used to in-

PHYSIOLOGY

vestigate the role of HCN4 channels in pacemaker generation and rate control. $Hcn4^{lox/lox,Cre}$ mice (defined from here on as ciHCN4-KO mice) were obtained by crossing homozygous $Hcn4^{lox/lox}$ mice carrying the loxP sites across exon 2 (Fig. 1 A–C; see *Materials and Methods* for further details) with heterozygous MerCreMer (MCM) mice carrying the Cre recombinase sequence downstream of the cardiac-specific α-myosin heavy chain promoter (αMHC). Cardiac-specific expression of the Cre activity was verified by crossing MCM transgenic mice with the reporter ROSA26-EYFP transgenic mice line. As shown in Fig. 1D, the reporter activity was detectable only in cardiac tissues.

Induction of HCN4 Knockout Causes Development of Deep Bradycardia and AV Block. We measured the ECG activity in freely moving animals by telemetry. Fig. 2A shows representative heart rate recordings from a control and a ciHCN4-KO animal during Tam treatment. In the ciHCN4-KO animal, knockout of HCN4 cumulatively induced by daily tamoxifen injections (Fig. 2A, arrows) was associated with a progressive development of severe bradycardia (from 550 to <200 bpm) until death intervened after the fourth injection; only a minor heart rate reduction was observed in the control animal undergoing the same treatment. Rate recordings as in Fig. 2A were collected from $n = 14$ control and $n = 14$ ciHCN4-KO mice to determine the mean time
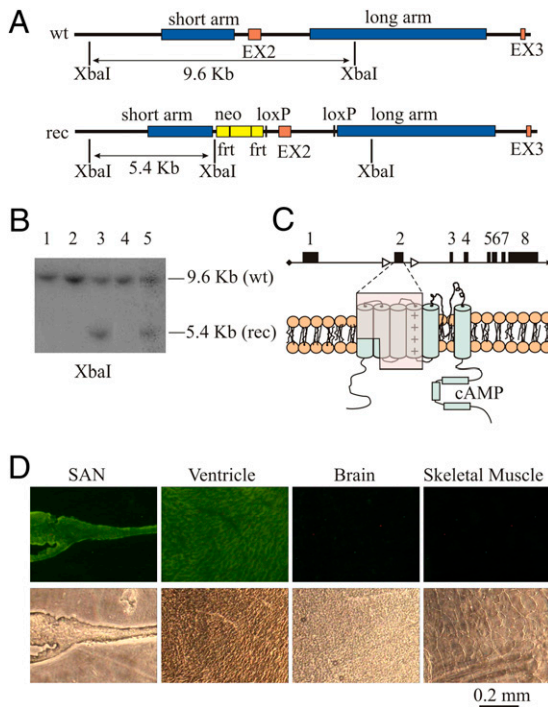
Fig. 1. Generation of $Hcn4^{lox/lox,Cre}$ transgenic mice and cardiac specificity of the knockout process. (A) Structure of the wild type (wt) and recombinant (rec) $Hcn4$ alleles. The long and short arms of homology used for the recombination process and the loxP sites and the neomycin resistance cassette (neo) used for cell selection are shown. (B) Southern blot analysis of XbaI restriction fragments of DNA extracted from five clones; the two bands in lanes 3 and 5 confirm the presence of one recombinant allele. (C) The Cre-induced removal of exon 2 (*Upper*) eliminates a large part of the protein (*Lower*, shaded area) and generates a frameshift leading to an early stop codon three residues downstream of R262; this results in a DNA sequence coding for a truncated protein including only the HCN4 N terminus. (D) Tissue slices obtained from sinoatrial node (SAN), ventricle, brain, and skeletal muscle extracted from an MCM, ROSA26-EYFP transgenic mouse at day 5 of Tam treatment. The expression of enhanced yellow fluorescent protein (EYFP) is restricted to the SAN and the ventricle as expected for a cardiac conditional activation of Cre-recombinase. Each fluorescent image (*Upper* panels) is paired with the corresponding bright-field image (*Lower* panels). Further details are in *SI Materials and Methods*.
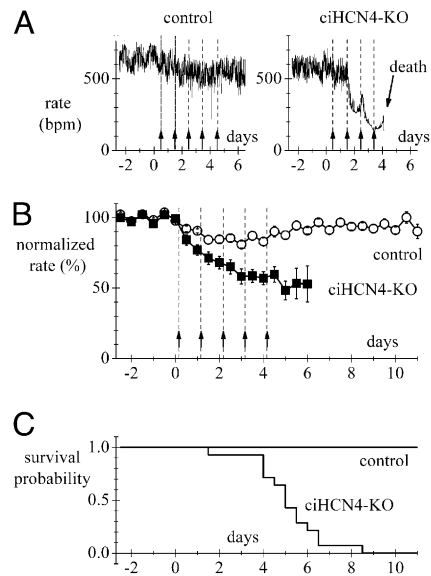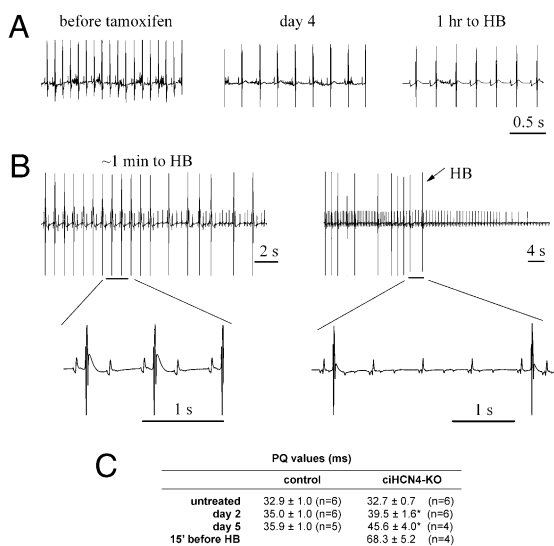

Fig. 2. Knockout of HCN4 induces deep bradycardia and is lethal. (A) Representative traces of telemetric heart rate recorded from freely moving control (*Left*) and ciHCN4-KO mice (*Right*). Administration of Tam is indicated by arrows; 8:00 AM of the day of the first injection was conventionally set as time 0. (B) Mean time courses of normalized heart rates for control ($n = 14$) and ciHCN4-KO ($n = 14$) mice during Tam treatment. For each day, two data points were calculated by averaging rates in the intervals 8:00–10:00 AM and 8:00–10:00 PM. These values where then normalized to a baseline heart rate, corresponding to the average heart rate in the same time periods collected for 2–5 d before initiation of the Tam treatment. (C) Kaplan–Meier survival curves for the same sets of control and ciHCN4-KO mice as in B, illustrating the rapid decay of survival probability for ciHCN4-KO mice.

courses shown in Fig. 2B. A progressive, substantial decrease of rate was observed in ciHCN4-KO but not in control mice. The mean heart rate before Tam treatment was 584.3 ± 17.5 bpm and 545.5 ± 18.1 bpm for control and ciHCN4-KO mice, respectively. The mean heart rate decreased by 32.0% at day 2 and by 47.1% at day 6 of treatment; differences between control and ciHCN4-KO mean rates were significant at all times starting from day 1 ($P < 0.05$). A minor rate reduction was recorded in control animals, which, however, recovered within 10 d, suggesting an unspecific effect of tamoxifen. The survival probability curves in Fig. 2C illustrate the high degree of lethality of Tam treatment for ciHCN4-KO mice: although all control animals survived, none of the 14 ciHCN4-KO mice analyzed by telemetry lived more than 8.5 d. The mean survival time for the ciHCN4-KO mice was 4.87 ± 0.42 d ($n = 14$).

The observation that all ciHCN4-KO animals died during progression of HCN4 knockout prompted a more detailed analysis of the ECG activity recorded during the last phases of the Tam procedure. In Fig. 3A, sample ECG traces recorded from a ciHCN4-KO mouse before (*Left*), at day 4 (*Center*), and at day 4.77 of Tam treatment (≈1 h before heart block, *Right*) reveal that, together with the development of deep bradycardia, a prolongation of the PQ interval (distance between P wave and Q wave of QRS complex), typical of first-degree AV block, also took place (PQ = 32.2, 51.2, and 85.3 ms, *Left* to *Right*). As the rate progressively decreased, the AV block became more severe and evolved into a second-degree block characterized first by a 2:1 (Fig. 3B, *Left*) and then by a 4:1 (Fig. 3B, *Right*) or higher conduction ratio. Two-to-one conduction ratios were observed in this mouse starting at about 7 min before heart block. Complete AV block (heart block, HB) in the absence of accessory ventricular rhythm eventually led to heart arrest and death of the animal.

Atrial activity persisted throughout AV block. Evidence similar to that in Fig. 3 was apparent in the ECGs from all Tam-treated ciHCN4-KO animals where this was investigated ($n = 5$).
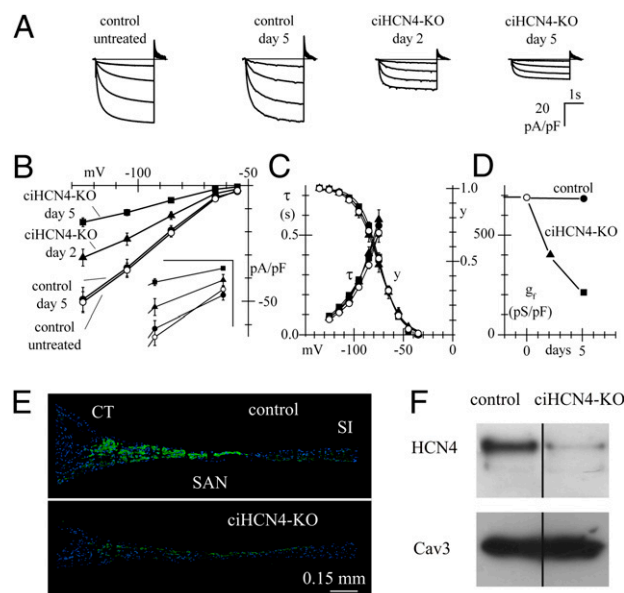
A before tamoxifen   day 4   1 hr to HB

0.5 s

B ~1 min to HB   HB

2 s   4 s

1 s   1 s

C

	PQ values (ms)	
	control	ciHCN4-KO
untreated	32.9 ± 1.0 (n=6)	32.7 ± 0.7 (n=6)
day 2	35.0 ± 1.0 (n=6)	39.5 ± 1.6* (n=6)
day 5	35.9 ± 1.0 (n=5)	45.6 ± 4.0* (n=4)
15' before HB		68.3 ± 5.2 (n=4)

Fig. 3. Development of heart block (HB) in ciHCN4-KO mice. (*A*) Typical telemetric ECG recordings from a ciHCN4-KO mouse before the first Tam injection (452.4 ± 0.7 bpm), at day 4 (240.8 ± 1.3 bpm), and 1 h before HB and death of the animal (day 4.77, 210.2 ± 0.5 bpm). (*B*) Traces recorded 1 min (*Left*) and just before HB (*Right*), indicating the progression of second-degree AV block from 2:1–4:1 and higher conduction ratios. Heart arrest occurred shortly after the last QRS complex of the ECG recorded (*Right*). Selected portions of traces are shown on an expanded time scale. (*C*) Mean PQ values measured during the Tam procedure in control and ciHCN4-KO mice. For each mouse, a mean PQ was measured from 3-min-long recordings, and values in the table were averaged over the number of mice indicated (*$P < 0.05$ vs. day-matched control).

The average time of appearance of the 2:1 conduction ratio in ciHCN4-KO animals was 4.50 ± 0.30 d ($n = 5$). Mean PQ intervals from control and ciHCN4-KO mice at different times of Tam treatment are listed in Fig. 3*C*.

I_f Current and HCN4 Protein Expression in Single Cells and Intact SAN Tissues from ciHCN4-KO Mice. We analyzed the effects of HCN4 knockout on the properties of the I_f current by patch-clamp experiments in cells isolated from the SAN. At all voltages investigated, although Tam treatment did not affect the current in cells from control mice (*t* test, $P > 0.05$, Fig. 4*B*), the mean I_f current densities measured in SAN cells isolated from ciHCN4-KO animals at day 2 and day 5 of Tam treatment were different from each other and were lower than those of cells isolated from control mice (one-way ANOVA followed by Fisher test, 0.05 significance; Fig. 4 *A* and *B* and Table S1). We also measured the voltage dependence of activation and activation time constants of I_f in SAN cells from the four types of mice (Fig. 4*B*). As apparent from Fig. 4*C*, all curves overlapped and were not significantly different. Because the kinetic properties of I_f (Fig. 4*C*) and capacitance (Table S1) did not vary, the observed reduction of I_f density implies a reduced membrane channel density of HCN4 in ciHCN4-KO mice. The time-dependent decrease of I_f conductance (g_f) in ciHCN4-KO cells is shown in Fig. 4*D*.

To verify whether the I_f conductance decrease of Tam-treated ciHCN4-KO mice (Fig. 4 *B* and *D*) correlates with tissue protein, we investigated the expression of HCN4 in the SAN using immunofluorescence and Western blot analysis. SAN tissue slices immunolabeled with primary antibodies against mHCN4 proteins from a control and a ciHCN4-KO mouse (day 5 of Tam treatment) are shown in Fig. 4*E*. While positive staining was apparent in the central region of the slice from the control mouse, in agreement with established evidence for HCN4 expression in the central node area (4, 5, 20), a much reduced labeling was detected in the ciHCN4-KO mouse. Similar evidence for strongly reduced HCN4 protein expression in Tam-treated ciHCN4-KO mice was

A control untreated   control day 5   ciHCN4-KO day 2   ciHCN4-KO day 5

20 pA/pF   1s

B   mV -100   -50

ciHCN4-KO day 5
ciHCN4-KO day 2
control day 5
control untreated

pA/pF
-50

C τ (s)   pA/pF   τ   y   mV -100   -50

D control   ciHCN4-KO g_f (pS/pF)   0 days 5

E CT   control   SI   SAN   ciHCN4-KO   0.15 mm

F control ciHCN4-KO   HCN4   Cav3

Fig. 4. Reduction of HCN4 expression in pacemaker cells and tissue from ciHCN4-KO mice. (*A*) Representative I_f traces (normalized to cell capacitance) during steps to −65/−125 mV (20-mV intervals, holding potential −35 mV) from SAN cells isolated from a control and a ciHCN4-KO mouse at various times during the Tam procedure. (*B*) Mean steady-state current/voltage (I/V) curves recorded in control mice before (open circles, $n = 44/9$ cells/mice) and at day 5 (solid circles, $n = 42/8$) and in ciHCN4-KO mice at day 2 (solid triangles, $n = 32/5$) and day 5 of Tam treatment (solid squares, $n = 42/7$). (*Inset*) Data at −55 and −65 mV on an expanded scale (vertical bar 5 pA/pF; horizontal bar 10 mV). At all voltages, means of I_f current density of control untreated and control day 5 mice were not significantly different (*t* test, $P > 0.05$), and data were pooled together for further statistical analysis. Means of I_f current density from control, ciHCN4-KO day 2, and ciHCN4-KO day 5 mice were compared by one-way ANOVA followed by Fisher test (0.05 significance level), which showed that, for each voltage, the ciHCN4-KO day 2 mean is significantly different from the ciHCN4-KO day 5 mean and that both are significantly different from the control mean. (*C*) Mean I_f activation (y) and activation time constant (τ) curves measured in cells from the same groups as in *B*. Data points of activation curves were fitted with the Boltzmann equation. Half-activation voltages and inverse-slope factors, respectively, were the following: −75.0 mV, 11.2 mV (control untreated, $n = 30$); −75.1 mV, 11.1 mV (control day 5, $n = 19$); −74.2 mV, 10.1 mV (ciHCN4-KO day 2, $n = 15$); and −76.0 mV, 11.7 mV (ciHCN4-KO day 5, $n = 11$). Time constant curves were the mean from $n = 15$, $n = 17$; $n = 12$ and $n = 7$ for the same categories above, respectively. (*D*) Mean normalized I_f conductance (g_f) measured from the data in *B* as the I/V slope in the interval −105/−125 mV. (*E*) HCN4 immunolabeling (green) of intercaval tissue slices obtained from representative control and Tam-treated ciHCN4-KO mice. Nuclei are labeled with DAPI (blue). CT, crista terminalis; SI, septum interatrialis. (*F*) Western blot of total SAN protein extracts (30 μg/lane) showing expression of the HCN4 protein in control and 4.5-d Tam-treated ciHCN4-KO mice. Cav3: loading control.

provided by immunolabeling experiments in single SAN cells (Fig. S1). Accordingly, Western blot analysis of SAN protein extracts revealed a strong positive HCN4 signal in control animals, whereas the signal from ciHCN4-KO animals was just above the detection threshold (Fig. 4*F*). These data confirm that Tam-induced knockout of HCN4 affects only the membrane channel density. Tissue labeling of HCN1 and HCN2 (Fig. S2) indicates no detectable protein signals in both control and ciHCN4-KO mice; this also implies that expression of these two isoforms does not increase in knockout animals relative to wild type.
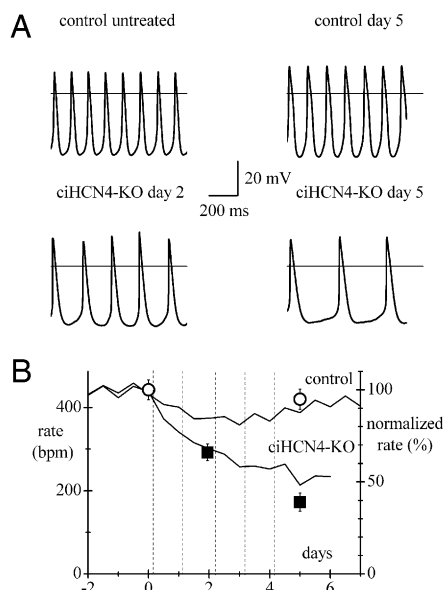
Spontaneous Rate of Single SAN Myocytes from ciHCN4-KO Mice. We next proceeded to verify whether the bradycardia observed in Tam-treated ciHCN4-KO animals derived from a reduced automaticity of single pacemaker cells. SAN cells were isolated from untreated control and control mice after 5 d of Tam or vehicle treatment and

PHYSIOLOGY

from ciHCN4-KO mice after 2 or 5 d of Tam treatment. Cells from all types of mice exhibited spontaneous activity (Fig. 5A). Mean spontaneous rates from the four categories of mice in Fig. 5A are plotted in Fig. 5B at various times during the Tam procedure (Table S2). The frequency of cells from control mice was not significantly reduced, whereas that from ciHCN4-KO mice dropped significantly after 2 and 5 d of Tam treatment ($P < 0.05$).

To compare these results with in vivo telemetric measurements, we normalized the data (right y axis in Fig. 5B) and superimposed the normalized rate curve from Fig. 2B. Clearly, the time courses of rate from single cells and from freely moving animals do not differ substantially, confirming that the bradycardia induced by ciHCN4 knockout results from a slower spontaneous rate of SAN cells. Sample video recordings of the spontaneous activity of representative intact tissues and SAN cells from control and ciHCN4-KO mice (day 5 of Tam treatment) are shown in Movie S1 and Movie S2, respectively.

Response to β-Adrenergic Receptor Stimulation. To explore the effects of the loss of HCN4 protein on β-adrenergic receptor (β-AR) modulation of rate, we used telemetry to measure frequency responses to i.p. injection of isoproterenol (Iso) in control and ciHCN4-KO mice. To ensure a low level of HCN4 expression, we selected Tam-treated ciHCN4-KO mice with a frequency stably lower than 50% of their mean basal rate. Sample recordings shown in Fig. 6A (Left and Center) show that in both control and ciHCN4-KO mice injection of Iso (0.1 mg/kg) induced rate acceleration. Mean data calculated in $n = 5$ control and in $n = 7$ ciHCN4-KO mice indicate that although the rate change (Δrate = maximal rate − basal rate) did not vary between the two groups (Δrate = 192.9 ± 17.7 bpm vs. 184.7 ± 8.5 bpm, $P > 0.05$), ciHCN4-KO animals failed to attain the same maximal rate reached by control animals (Fig. 6A, Right) (mean values in Table

S3). We then investigated the effect of Iso on the spontaneous activity of control and ciHCN4-KO cells. As shown in the representative action potential recordings of Fig. 6B, 1 μM Iso accelerated the spontaneous rate in both control and ciHCN4-KO cells (Fig. 6B, Left and Center).

In agreement with the telemetry data in Fig. 6A, Iso-induced rate acceleration was similar in control and ciHCN4-KO cells (Fig. 6B, 119.9 ± 33.4 bpm vs. 143.4 ± 20.6 bpm, $P > 0.05$), whereas maximal values of rate under stimulation were higher for control than for ciHCN4-KO cells ($P < 0.05$) (mean values in Table S4).
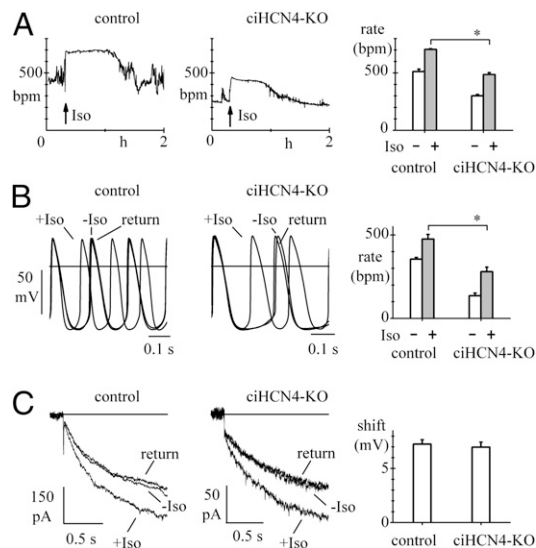
In a previous HCN4 KO model, the residual I_f current was reported not to respond to Iso (16). We compared the I_f response to Iso in SAN cells isolated from Tam-treated ciHCN4-KO vs. control mice, and as shown in Fig. 6C, the response was not modified in ciHCN4-KO mice. Iso (1 μM) shifted the I_f activation curve by an average 7.2 ± 0.4 mV ($n = 12$) in cells from control and 7.0 ± 0.5 mV ($n = 7$) in cells from ciHCN4-KO mice ($P > 0.05$).

These results suggest that, although strongly reduced in size, the residual I_f still retains the ability to contribute to β-AR–induced rate modulation in ciHCN4-KO mice. Also, the contribution to rate acceleration of mechanisms other than I_f is likely to be amplified in conditions of reduced HCN4 expression.

Discussion

Our results show that cardiac-specific reduction of the *Hcn4* gene in adult animals leads to the development of severe sinus bradycardia, with a slowing of rate of ~50% after five daily Tam injections (Fig. 2B), and to the progression of AV block, eventually leading to heart block and death of the animal (Figs. 2 and 3).

Patch-clamp investigation of single SAN cells showed a substantial, progressive decrease of the size of the I_f current in ciHCN4-KO animals, without alteration of its kinetic properties

Fig. 5. Effects of HCN4 knockout on spontaneous activity of single SAN cells. (A) Sample action potentials recorded from SAN cells isolated from control mice before and at day 5 (Upper panels) and from ciHCN4-KO mice at day 2 and day 5 of Tam treatment. Rates from 2- to 4-s-long recordings were 434.4, 436.4, 288.1, and 170.4 bpm, respectively. (B) Mean rates from cells of the same mouse categories as in A plotted against the time of recording. Control rates were 444.5 ± 23.7 bpm (untreated, $n = 15/8$ cells/mice) and 422.0 ± 24.5 bpm (5-d exposure to Tam or vehicle, $n = 12/6$ cells/mice); ciHCN4-KO rates were 293.6 ± 20.2 bpm (day 2, $n = 20/6$ cells/mice) and 173.1 ± 21.6 bpm (day 5, $n = 26/9$ cells/mice). All values were significantly different from each other ($P < 0.05$) except control vs. control day 5. The y axis on the right represents normalized values. The time courses of mean normalized telemetric heart rate of control and ciHCN4-KO mice from Fig. 2B are also plotted for comparison.

Fig. 6. Response to β-AR stimulation. (A) Representative telemetry recordings from a control mouse (Left) and a ciHCN4-KO mouse (Center) at the fifth day of Tam treatment showing rate responses to the injection of Iso (arrows; Materials and Methods). (Right) Mean rates before and after Iso from control treated ($n = 5$) and ciHCN4-KO mice ($n = 7$). (B) Representative traces showing acceleration of spontaneous activity of two SAN cells from a control treated (Left) and a ciHCN4-KO mouse (center) exposed to 1 μM Iso. (Right) Mean spontaneous rates before and after Iso in cells from control treated ($n = 6$) and ciHCN4-KO mice ($n = 10$). (C) Action of 1 μM Iso on I_f recorded at −75 mV in SAN cells isolated from typical control (Left) and ciHCN4-KO mice (Center). (Right) Mean shifts of the I_f activation curve caused by 1 μM Iso in cells from control treated mice ($n = 12$) and ciHCN4-KO mice ($n = 7$). Asterisks in A and B indicate significant differences ($P < 0.05$). Records in B and C are before, during, and after Iso as indicated.

(Fig. 4). The time course of bradycardia measured by telemetry and that of the spontaneous rate of ciHCN4-KO SAN cells isolated at different stages of Tam treatment were similar (Fig. 5B), indicating that both processes are a direct consequence of reduced HCN4 channel contribution to pacemaking. Finally, immunofluorescence and Western blot analysis confirmed a strongly reduced expression of HCN4 protein in the SAN region of ciHCN4-KO mice after Tam treatment (Fig. 4 E and F).

Adult HCN4 KO mouse models have previously been developed (16, 17). These models were inducible but were not generated by cardiac-specific recombination. In one study (16), the recombination of the floxed *Hcn4* locus was obtained by use of the ubiquitous inducible CAGG-Cre, resulting in global HCN4 knockout. In another study (17), the Tam-inducible CreERT2 construct was placed under the control of the *Hcn4* promoter. In both models, therefore, the *Hcn4* gene was knocked out in all *Hcn4*-expressing cells accessible to tamoxifen. Because HCN4 channels are widely expressed in central and peripheral neurons (18, 19) as well as in cardiac myocytes, the phenotypic properties of HCN4 knockout mice in these models cannot be assumed to originate from the exclusive effects on the cardiac I_f current, even if in theory one would expect more severe phenotypic consequences from a general loss of HCN4.

In our model, on the other hand, the Cre recombinase expression was under the control of the cardiac-specific αMHC promoter, which ensured restriction of HCN4 knockout to cardiac tissue (Fig. 1D). The main finding obtained with previous in vivo HCN4 KO models (16, 17) was the occurrence of frequent sinus pauses in between bursts of normal activity, but impairment of the cardiac function in these animals was not critical enough to be lethal. In fact, these mice had mean basal heart rates nonsignificantly different from those of wild-type mice and normally responsive to β-AR stimulation. This behavior cannot be easily reconciled with the observation that a large fraction of single SAN cells [45% (17) to 90% (16)] isolated from the KO mice do not show spontaneous activity. In contrast with previous data, inducible and cardiac-specific knockout of HCN4 in our mouse model led to profound bradycardia and death caused by heart block (Fig. 2). In agreement with in vivo results, single SAN cells isolated from our ciHCN4-KO mice always displayed a relatively regular, if slow, spontaneous activity (Fig. 5 and Movie S2).

We have no straightforward explanation for the differences in heart and single-cell automaticity between our mouse model and previous inducible models because the degree of I_f reduction observed in SAN cells is comparable [68.5% at −125 mV after 5 d of Tam treatment (Fig. 4) vs. 75% (16) and 79% (17)].

We can only speculate that part of these differences may arise from differences in cardiac specificity of HCN4 knockout and from the observation that, whereas in our experiments the position of the I_f activation curve was relatively depolarized [$V_{1/2}$ was about −75 mV (Fig. 4)], values reported previously are substantially more negative [−91.2 mV (16) and −93.5 mV (17)]. Although it is known that the position of the activation curve is strongly affected by a variety of elements and conditions (18, 19), we have no explanation for these differences. It should be noted in any case that a more depolarized activation range is bound to make spontaneous activity more dependent upon HCN4 knockout.

Our ciHCN4-KO animals preserved the rate response to β-AR stimulation (Fig. 6A) and the Iso-induced rate acceleration was similar in wild-type and ciHCN4-KO mice, although the maximal rate attained by the latter group was clearly reduced. When the effect of Iso on rate was investigated in single cells, similar results were obtained (Fig. 6B). Indeed, the HCN4 knockout process did not impair Iso-induced rate modulation but affected the maximal rate of ciHCN4-KO cells. The effects of Iso stimulation had also been investigated in previous HCN4 knockout models. Results obtained in vivo have shown that the response to Iso did not differ from that elicited in wild-type mice (16, 17). In vitro results from single cells have confirmed the permanence of modulation by noting that Iso rescued spontaneous activity in silent cells (16). Finally, when the modulation of Iso was investigated on the residual I_f, we found no differences between ciHCN4-KO and control cells, a condition not verified in previous models.

The β-adrenergic modulation of rate has also been evaluated in a transgenic mouse expressing a human mutated HCN4 (hHCN4-573×) protein, which lacks the cAMP-binding site (21). Interestingly, this mouse model displays a basal bradycardia (figure 4 of ref. 21), and the effects of Iso stimulation are similar to those observed in our experiments because the maximal rate elicited by Iso was less than that observed in wild-type mice. Although the expression of an exogenous, mutated human gene in the mouse model by Alig et al. (21) is substantially different from our *Hcn4* gene knockout approach, the very negative, nonphysiological activation range of I_f that they report implies loss of functional I_f expression and contribution to activity similar to our model. Taken together, our results and those of Alig et al. (21) indicate that the integrity of the HCN4 current to pacemaking is essential because it is required to establish both the basal heart rate and the maximal firing rate upon Iso stimulation. The fact that Alig et al.'s model (21), in contrast to ours, is not lethal remains unexplained. While in their model the Iso-induced rate acceleration cannot be determined by the I_f current, this is not the case in our model, where a Iso-modulated, residual I_f current is still present after partial loss of HCN4 channels. In our model, the I_f increase by Iso will in fact be smaller in ciHCN4-KO than in control mice, but because the basal frequency is also lower, the I_f increase required to change it will be proportionally reduced. In addition, the contribution of mechanisms other than I_f, which participate in the rate acceleration by modifying the last fraction of diastolic depolarization, namely Ca^{2+} currents and the Na^+-Ca^{2+} exchanger (1), will likely play a more important role.

Our investigation indicates that HCN4 knockout induces a smooth development of bradycardia but does not lead to the abolishment of SAN activity, which is still present at the time of death of the animal. Tam-treated ciHCN4-KO mice live an average of 4.9 d (Fig. 2), and at the time of death HCN4 channels are not fully removed from SAN cells, as indicated by the evidence that after 5 d of Tam treatment about 30% of the original I_f is still expressed (Fig. 4 A, B, and D). Residual I_f could also result from the contribution of HCN isoforms other than HCN4, in particular HCN1 and HCN2. This, however, appears less likely because the I_f reduction did not involve changes in kinetics (Fig. 4), while the HCN1 and HCN2 isoforms have kinetic properties distinctly different from those of HCN4 (19). Additional evidence in support of this conclusion derives from our preliminary immunofluorescence data indicating no detectable protein level of either HCN1 or HCN2 proteins in SAN strips from both control and ciHCN4-KO mice (Fig. S2). This also demonstrates lack of any compensatory mechanism for HCN4 reduction. The presence of a residual I_f current, also reported in previous models (15–17), agrees with the permanence of regular, if progressively slower, supraventricular rhythm throughout the period of Tam treatment up to the occurrence of heart block (Fig. 3).

The death of ciHCN4-KO animals is a sudden event and a consequence of the lack of idioventricular rhythm and AV block. The absence of sustained idioventricular rhythm after AV block agrees well with the notions that in mice HCN4 channels are highly expressed also in physiological conditions in the His-Purkinje system (22) and that the MHC promoter is active in the cardiac conduction tissue (23).

Preliminary data from our ciHCN4-KO model indeed confirm the presence of HCN4 in the AVN and show a reduction of current (about 63% after 5 d of Tam treatment; Fig. S3) comparable with that in the SAN. Our data also show that the HCN4 current in the AVN is about 50% of that in the SAN, in agreement with the established notion that I_f is expressed in the AVN (8, 24, 25) at a lower density than in the SAN and as expected with the slower intrinsic rate (8, 25, 26). It therefore appears paradoxical that the effects of HCN4 knockout should be more deleterious in the AVN, where pacemaker channels are fewer than in the SAN.

It is interesting to note that, according to previous data, block of I_f generates a larger response in AVN than in SAN myocytes. For example, superfusion of 3 μM ZD7288, a dose known to block the I_f current by 73%, completely stopped the activity of mouse AVN cells, but it reduced by only 48% the cycle length in SAN cells (25). To interpret this apparent paradox, it was proposed that

a longer cycle time in AVN cells may involve a larger inward I_f during diastolic depolarization (25). However, this explanation cannot be applied to our data because SAN and AVN cycle times are identical in in vivo conditions. It is possible, on the other hand, that different contributions from components other than I_f flowing during diastolic depolarization determine a different sensitivity to I_f inhibition. For example, given the high voltage dependence of I_f activation, a more negative level of maximum diastolic potential in AVN cells, if present, could be associated with a higher fractional degree of I_f activation during diastole and hence with a higher susceptibility to block. Although the above explanation is speculative, the observation that the AVN is more sensitive than the SAN to f-channel inhibition when tested in isolated myocytes or in fully independent in vivo recordings from ciHCN4-KO animals remains a significant and intriguing result that awaits further confirmation and interpretation.

The observation that signal conduction through the AVN is impaired upon HCN4 knockout can be the consequence of the remodeling of ion channel expression of the heart, but it could also more specifically suggest a potential, previously unsuspected role of HCN4 channels in AVN function.

In conclusion, contrary to previous data, the present work shows that induction of cardiac-specific knockout of HCN4 causes progressive bradycardia and heart block and is lethal. Thus, loss of HCN4 in the adult mouse is not compatible with life. Our results confirm the relevance of HCN4 channels in controlling cardiac rate; they also open perspectives of clinical relevance in the investigation of the potential role of HCN4/f channels in pathologies involving the function of the AVN and the cardiac conduction system.

Materials and Methods

Generation of Inducible and Cardiac-Specific HCN4 KO Mice and Tamoxifen Administration. A 129SvEv PAC library was screened using the *Hcn4*-specific primers 5′ CTGGTATGGGGACTTTCAC 3′ and 5′ CAACAGCATCGTCAGGTCC 3′ and the following amplification profile: one cycle at 96 °C for 10 min; 40 cycles at 96 °C, 45 s; 60 °C, 45 s 72 °C, 45 s; and one cycle at 72 °C for 7 min. The positive clone obtained from the library was digested with EcoRV+EcoRI, and two fragments of 2.5 kb (corresponding to the short arm of homology) and 9 kb (corresponding to exon 2 and the long arm of homology) (Fig. 1A) were subcloned in a Bluescript plasmid and used for the production of the targeting vector. A fragment of 2.5 kb comprising exon 2 was cloned between loxP sites of the empty targeting vector (construct 1), which contained a neomycin resistance (Neo) cassette flanked by Flb recombination target (Frt) sites.

The short arm of homology was blunted and cloned into the XhoI site of construct 1 (construct 2). This was subsequently modified by introducing a BamHI/EcoRI-containing adapter into the NotI/SacII sites of construct 2. This allowed the directional cloning of the 6.2 kb long arm into the BamHI/EcoRI sites (construct 3). This vector was linearized by restriction with SacII and electroporated into 129SvEv ES cells. Clones resistant to G418 selection were digested with XbaI and screened by Southern blot using a probe external to the short arm of homology. Southern blot analysis was performed according to standard procedures (27). Five positive clones, showing both the 9.6-kb wild-type and the 5.4-kb recombinant bands, were identified within 180 screened clones and further checked with a probe external to the long arm of homology. In Fig. 1B, two positive and three negative clones are shown. Positive clones were injected into C57BL/6 blastocysts and chimeras were obtained. High-chimerism males were mated with C57BL/6 wild-type mice to assess germ-line transmission. Mice from F1 were bred to Flp transgenic mice to remove the Neo cassette and finally reduced to homozygosity. Homozygous *Hcn4*$^{lox/lox}$ mice were finally crossed with MCM transgenic mice (28) heterozygous for the *Hcn4* floxed allele (*Hcn4*$^{+/lox;Cre}$) to obtain mice with the appropriate *Hcn4*$^{lox/lox;Cre}$ genotype.

Knockout was induced by i.p. injections of Tamoxifen (Tam, Sigma Aldrich, 0.2 mg/g) for 5 consecutive days in adult (>60 d-old) *Hcn4*$^{lox/lox;Cre}$ male and female mice. The injections were administered always at 12:00 AM, and the first injection was conventionally defined as occurring at day 0. Tam was dissolved in corn oil with 10% ethanol at a concentration of 20 mg/mL and prepared daily. For additional details, see *SI Materials and Methods*.

Cardiac Telemetry. For details, see *SI Materials and Methods*.

Single-Cell Electrophysiology. For details, see *SI Materials and Methods*.

Western Blot and Immunofluorescence. For details, see *SI Materials and Methods*.

Statistical Analysis. Statistical differences were determined at the $P < 0.05$ level by Student's t tests or ANOVA. All values are given as mean ± SEM.

1. Lakatta EG, DiFrancesco D (2009) What keeps us ticking: A funny current, a calcium clock, or both? *J Mol Cell Cardiol* 47:157–170.
2. Mangoni ME, Nargeot J (2008) Genesis and regulation of the heart automaticity. *Physiol Rev* 88:919–982.
3. Altomare C, et al. (2003) Heteromeric HCN1-HCN4 channels: A comparison with native pacemaker channels from the rabbit sinoatrial node. *J Physiol* 549:347–359.
4. Brioschi C, et al. (2009) Distribution of the pacemaker HCN4 channel mRNA and protein in the rabbit sinoatrial node. *J Mol Cell Cardiol* 47:221–227.
5. Tellez JO, et al. (2006) Differential expression of ion channel transcripts in atrial muscle and sinoatrial node in rabbit. *Circ Res* 99:1384–1393.
6. Chandler NJ, et al. (2009) Molecular architecture of the human sinus node: Insights into the function of the cardiac pacemaker. *Circulation* 119:1562–1575.
7. Shi W, et al. (1999) Distribution and prevalence of hyperpolarization-activated cation channel (HCN) mRNA expression in cardiac tissues. *Circ Res* 85:e1–e6.
8. Marionneau C, et al. (2005) Specific pattern of ionic channel gene expression associated with pacemaker activity in the mouse heart. *J Physiol* 562:223–234.
9. Moosmang S, et al. (2001) Cellular expression and functional characterization of four hyperpolarization-activated pacemaker channels in cardiac and neuronal tissues. *Eur J Biochem* 268:1646–1652.
10. DiFrancesco D (2010) Funny channel-based pacemaking. *Heart Rhythm* 7:276–279.
11. Espinoza-Lewis RA, et al. (2009) Shox2 is essential for the differentiation of cardiac pacemaker cells by repressing Nkx2-5. *Dev Biol* 327:376–385.
12. Wiese C, et al. (2009) Formation of the sinus node head and differentiation of sinus node myocardium are independently regulated by Tbx18 and Tbx3. *Circ Res* 104:388–397.
13. Mommersteeg MT, et al. (2007) Molecular pathway for the localized formation of the sinoatrial node. *Circ Res* 100:354–362.
14. DiFrancesco D, Camm JA (2004) Heart rate lowering by specific and selective I(f) current inhibition with ivabradine: A new therapeutic perspective in cardiovascular disease. *Drugs* 64:1757–1765.
15. Stieber J, et al. (2003) The hyperpolarization-activated channel HCN4 is required for the generation of pacemaker action potentials in the embryonic heart. *Proc Natl Acad Sci USA* 100:15235–15240.
16. Herrmann S, Stieber J, Stöckl G, Hofmann F, Ludwig A (2007) HCN4 provides a 'depolarization reserve' and is not required for heart rate acceleration in mice. *EMBO J* 26:4423–4432.
17. Hoesl E, et al. (2008) Tamoxifen-inducible gene deletion in the cardiac conduction system. *J Mol Cell Cardiol* 45:62–69.
18. Robinson RB, Siegelbaum SA (2003) Hyperpolarization-activated cation currents: From molecules to physiological function. *Annu Rev Physiol* 65:453–480.
19. Biel M, Wahl-Schott C, Michalakis S, Zong X (2009) Hyperpolarization-activated cation channels: From genes to function. *Physiol Rev* 89:847–885.
20. Liu J, Dobrzynski H, Yanni J, Boyett MR, Lei M (2007) Organisation of the mouse sinoatrial node: Structure and expression of HCN channels. *Cardiovasc Res* 73:729–738.
21. Alig J, et al. (2009) Control of heart rate by cAMP sensitivity of HCN channels. *Proc Natl Acad Sci USA* 106:12189–12194.
22. Remme CA, et al. (2009) The cardiac sodium channel displays differential distribution in the conduction system and transmural heterogeneity in the murine ventricular myocardium. *Basic Res Cardiol* 104:511–522.
23. Dobrzynski H, et al. (2006) Expression of Kir2.1 and Kir6.2 transgenes under the control of the alpha-MHC promoter in the sinoatrial and atrioventricular nodes in transgenic mice. *J Mol Cell Cardiol* 41:855–867.
24. Noma A, et al. (1980) Slow current systems in the A-V node of the rabbit heart. *Nature* 285:228–229.
25. Liu J, et al. (2008) Role of pacemaking current in cardiac nodes: Insights from a comparative study of sinoatrial node and atrioventricular node. *Prog Biophys Mol Biol* 96:294–304.
26. Yuill KH, Hancox JC (2002) Characteristics of single cells isolated from the atrioventricular node of the adult guinea-pig heart. *Pflugers Arch* 445:311–320.
27. Sambrook J, Russel DW (2001) *Molecular Cloning: A Laboratory Manual* (Cold Spring Harbor Laboratory Press, Cold Spring Harbor, NY).
28. Sohal DS, et al. (2001) Temporally regulated and tissue-specific gene manipulations in the adult and embryonic heart using a tamoxifen-inducible Cre protein. *Circ Res* 89:20–25.